From February 2010 *High Frequency Electronics*

Electromagnetic Radiation From a Coated Cylinder with Two Arbitrary Axial Slots

By Muhammad A. Mushref
CEng, IEng, CITP

This paper provides an analysis of an axial slot antenna with two arbitrarily positioned slots, which might be used for Smart Antennas and Multiple Input Multiple Output (MIMO) systems

Electromagnetic radiation from coated circular cylinders with an axial slot is a traditional topic in wave theory. In the literature, numerous studies have previously examined the field characteristics from such structures. Investigations about the radiated field when two axial slots of arbitrary size and position exist are yet not considered.

A method was explained for determining the radiation patterns of an axial slot antenna on the surface of a metallic circular cylinder (Sinclair, 1948 [7]). For a slot of arbitrary shape an expression was derived for the external generated field. The far field was obtained by applying the method of steepest decent to the Fourier integrals in the solution (Silver and Saunders, 1950 [6]). Also, the radiation patterns of an axial slot in a dielectric coated circular cylinder were obtained with several comparisons to experimental results (Hurd, 1956 [3]).In addition, the fields produced by an arbitrary slot on a circular cylinder with a cocentric dielectric coating were reached. The far zone expressions were developed using a saddle–point method applied to the derived integrals (Wait and Mientka, 1957 [8]).

In this article, the TM field is investigated for two small axial slots in a thin circular cylinder coated with a lossless dielectric substance as shown in Figure 1. The cylinder is assumed to be a perfect electric conductor with radius a and with infinite extent along the z–axis. Two slots are axially cut on the surface of the cylinder with an angular opening of $2\theta_1$ and $2\theta_2$ located at $\phi = \phi_1$ and ϕ_2 respectively with respect to the ϕ–coordinate. Free space with permittivity ε_0 and permeability μ_0 is assumed region II. Also, the dielectric layer is assumed region I with radius b and characterized by ε and μ respectively. The dielectric material is assumed linear, homogenous and isotropic.

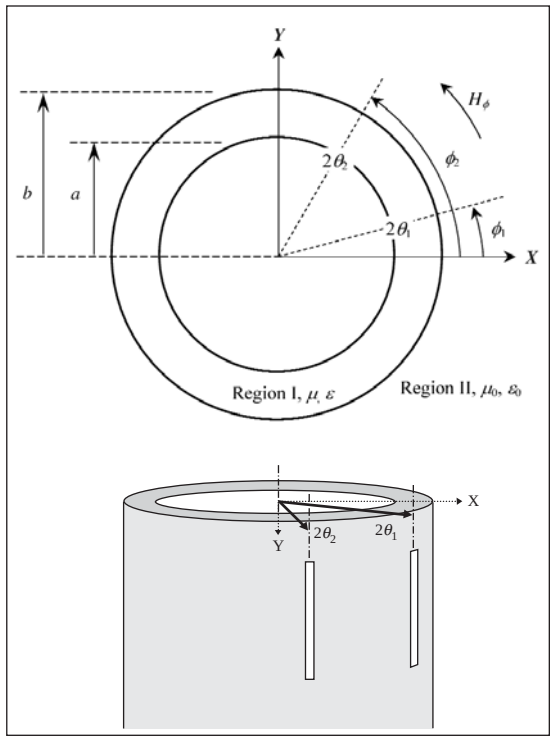

Figure 1 · Cross sectional view of the cylinder structure.

This article proposes an additional slot to the circular cylinder with arbitrary size and position which can be implemented to have different field patterns than the single slotted

cylinder. It is a very useful antenna structure that can be helpful in producing more than one radiation lobe at diverse directions and with different magnitudes.

Mathematical formulation and solution

Mathematical derivations start by solving the Helmholtz scalar wave equation in r and ϕ in the cylindrical coordinate system. Going after the separation of variables technique the result is the elementary wave function that can be Bessel functions multiplied by harmonic functions in r and ϕ respectively. Linear arrangements of the elementary wave functions are also a solution to the Helmholtz scalar wave equation and thus the summation over all possible values can be considered (Barrow, 1936 [1] and Harrington, 2001 [2]).

In region II the electric field radiates from the complete structure and as a result the Hankel function is assumed in r and multiplied by a complex exponential in ϕ as:

$$E_z^{II} = \sum_{n=-\infty}^{\infty} A_n H_n^{(2)}(k_0 r) e^{in\phi} \tag{1}$$

Similarly, in region I the electric field is represented by a summation of Bessel functions in r multiplied by a complex exponential in ϕ as:

$$E_z^{I} = \sum_{n=-\infty}^{\infty} \left\{ \alpha_n J_n(kr) + \beta_n Y_n(kr) \right\} A_n e^{in\phi} \tag{2}$$

In equations (1) and (2),

$$i = \sqrt{-1},\ J_n(x) \text{ and } Y_n(x)$$

are Bessel functions of the first and the second type respectively with order n and argument x. Also, $H_n^{(2)}(x)$ is the outgoing Hankel function of the second type with order n and argument x. k and k_0 are the dielectric coating and free space wave numbers respectively given by $k = 2\pi / \lambda$ where λ is the wavelength. The coefficients A_n, α_n and β_n are the unknowns that should be determined by applying the boundary conditions.

According to Figure 1, the tangential electric and magnetic fields are continuous at $r = b$ for all ϕ and the tangential electric field is zero at $r = a$ for all ϕ except at the slots. Also, the electric field at the slot aperture is ϕ–dependent (Harrington, 2001 [2]). That is:

$$E_z^{I} = E_z^{II} \quad r = b \quad 0 \le \phi \le 2\pi \tag{3}$$

$$H_\phi^{I} = H_\phi^{II} \quad r = b \quad 0 \le \phi \le 2\pi \tag{4}$$

$$E_z^{I} = \begin{cases} E_{0p} \cos\left(\pi(\phi - \phi_p)/2\theta_p\right) & r = a \quad -\theta_p + \phi_p < \phi < \theta_p + \phi_p \\ 0 & r = a \quad Else \end{cases} \tag{5}$$

where E_{0p} is the amplitude, p is 1 and 2 and $H_\phi = (-i/\omega\mu)(\partial E_z / \partial r)$ (Wait, 1988 [9]).

In order to find α_n and β_n the boundary conditions in equations (3) and (4) are applied to the field equations in (1) and (2) using the relation (Mushref, 2005 [4]):

$$\int_0^{2\pi} e^{-im\phi} e^{in\phi} d\phi = \begin{cases} 2\pi & m = n \\ 0 & m \ne n \end{cases} \tag{6}$$

where both n and m are integers.

The coefficients α_n and β_n are then found as:

$$\alpha_n = \frac{\pi k b}{2}\left[H_n^{(2)}(k_0 b) Y_n'(kb) - t_r H_n^{(2)'}(k_0 b) Y_n(kb) \right] \tag{7}$$

$$\beta_n = \frac{-\pi k b}{2}\left[H_n^{(2)}(k_0 b) J_n'(kb) - t_r H_n^{(2)'}(k_0 b) J_n(kb) \right] \tag{8}$$

where the prime notation designates differentiation with respect to the argument. Also,

$$t_r = \sqrt{\mu_r / \varepsilon_r},\ \mu_r = \mu / \mu_0 \text{ and } \varepsilon_r = \varepsilon / \varepsilon_0.$$

From the boundary condition is equation (5) the A_n coefficients are found to be:

$$A_n = \frac{X_n^1 + X_n^2}{\alpha_n J_n(ka) + \beta_n Y_n(ka)} \tag{9}$$

where,

$$X_n^p = \frac{2E_{0p}\theta_p}{\pi^2 - 4\theta_p^2 n^2} e^{-in\phi_p} \cos(n\theta_p) \qquad p \text{ is 1 or 2} \tag{10}$$

The asymptotic expression of the Hankel function for large argument is given as (Hurd, 1956):

$$H_n^{(2)}(x) = i^n e^{-ix} \sqrt{\frac{2i}{\pi x}} = e^{-i\left(x - \frac{n\pi}{2} - \frac{\pi}{4}\right)} \sqrt{\frac{2}{\pi x}} \qquad x \to \infty \tag{11}$$

The radiated field in equation (1) can be evaluated at a far point using equation (9) as:

$$E_z^{II} = P(\phi) e^{-i(k_0 r - \pi/4)} \sqrt{\frac{2}{\pi k_0 r}} \tag{12}$$

where P(ϕ) is the far field pattern given by:

$$P(\phi) = \sum_{n=-\infty}^{\infty} i^n A_n e^{in\phi} \tag{13}$$

In addition, the antenna gain and the aperture conductance per unit length λ_0 for the two slotted cylinder are respectively found as (Richmond, 1989):

$$G(\phi) = \frac{\pi |P(\phi)|^2}{2\sum_{n=-\infty}^{\infty} |A_n|^2} \tag{14}$$

$$G_a / \lambda_0 = \frac{4\sum_{n=-\infty}^{\infty} |A_n|^2}{|E_{01} + E_{02}|^2} \tag{15}$$

The Poynting vector in the equatorial plane at a far point for $r \to \infty$ is given by the cross product of the electric and magnetic fields in the radial direction as (Harrington, 2001):

$$P_V = (E \times *H) \bullet \vec{a}_r = \left| E_z^{II} * H_\phi^{II} \right| \tag{16}$$

where the symbol * indicates the complex conjugate and $\vec{a}_r$ is a unit vector in the radial direction.

The power radiates from the structure in all ϕ and as a consequence, the total radiated power in the equatorial plane can be found from the relation:

$$P_{eq} = \int_0^{2\pi} P_V d\phi \tag{17}$$

Using equations (16) and (17) with equation (9), P_{eq} per unit length λ_0 can be obtained as:

$$P_{eq} / \lambda_0 = \frac{\sum_{n=-\infty}^{\infty} |A_n|^2}{\pi^2 \eta_0} \tag{18}$$

where,

$$\eta_0 = \sqrt{\mu_0 / \varepsilon_0} \approx 120\pi$$

is known as the intrinsic impedance of free space.

Numerical Results and Discussions

The correctness of the expressions derived above can be confirmed by several numerical computations. Due to the convergence of the summation, the results obtained are calculated for n from –30 to 30. Also, a slot size of $\theta_0 = \pi / 100$ is assumed for computing field characteristics.

The antenna gain and the aperture conductance per unit length λ_0 are compared to the single slot case in

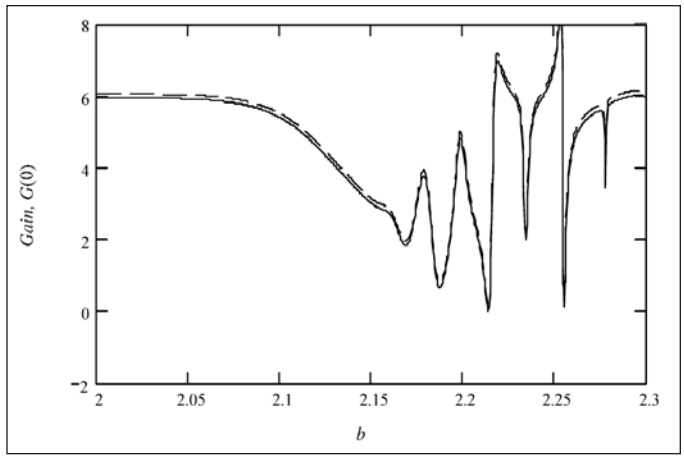

Figure 2(a) · Antenna gain versus coating thickness for $\varepsilon_r = 4$, $\mu_r = 1$ and $a = 2\lambda_0$, ——— (Richmond, 1989 (5)), - - - - calculated at $\phi = 0$ for $\phi_1 = 0$; $2\theta_1 = \theta_0$; $2\theta_2 = 0$.

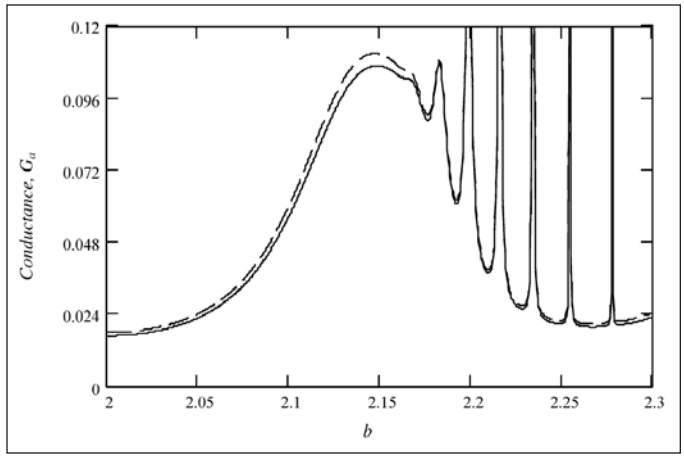

Figure 2(b) · Aperture conductance per unit length λ_0 versus coating thickness for $\varepsilon_r = 4$, $\mu_r = 1$ and $a = 2\lambda_0$, ——— (Richmond, 1989); - - - - calculated for one slot.

(Richmond, 1989). From equation (14), the antenna gain is plotted versus the coating thickness as shown in Figure 2(a) at the slot location for $\phi_1 = 0$, $2\theta_1 = \theta_0$, $2\theta_2 = 0$, $\varepsilon_r = 4$, $\mu_r = 1$ and $a = 2\lambda_0$. In addition, from equation (15) the aperture conductance is shown in Figure 2(b) versus the coating thickness for $\varepsilon_r = 4$, $\mu_r = 1$ and $a = 2\lambda_0$. As anticipated, great agreements can be observed from both curves which can support the correctness of the equations derived in this paper. Besides, convergence tests show that a sufficient number of terms are used for the infinite series produced in the solution.

Equations (14) and (15) for the two slots case are shown in Figure 3. The gain at $\phi = 0$ is plotted in Figure 3(a) for $\phi_1 = 0$, $2\theta_1 = 2\theta_2 = \theta_0$, $\phi_2 = \pi / 4$, $\pi / 2$ and π, $\varepsilon_r = 4$, $\mu_r = 1$ and $a = 2\lambda_0$. The shape is altered but without significant enhancements. One can notice that the gain is

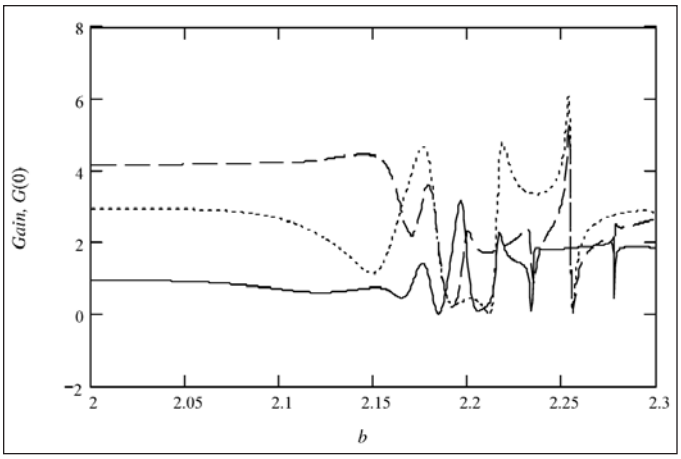

Figure 3(a) · Antenna gain at $\phi = 0$ versus coating thickness for $\varepsilon_r = 4$, $\mu_r = 1$, $a = 2\lambda_0$, $\phi_1 = 0$ and $2\theta_1 = 2\theta_2 = \theta_0$. ---- $\phi_2 = \pi / 4$; - - - - $\pi / 1$; · · · · π.

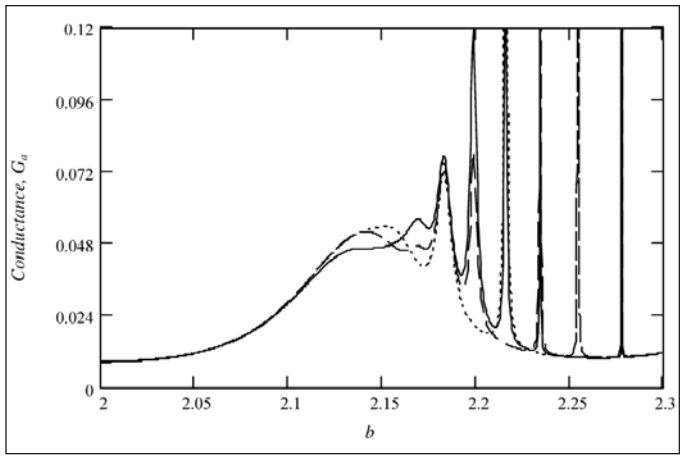

Figure 3(b) · Antenna conductance per unit length λ_0 versus coating thickness for $\varepsilon_r = 4$, $\mu_r = 1$, $a = 2\lambda_0$,$\phi_1 = 0$ and $2\theta_1 = 2\theta_2 = \theta_0$. ---- $\phi_2 = \pi / 4$; - - - - $\pi / 1$; · · · · π.

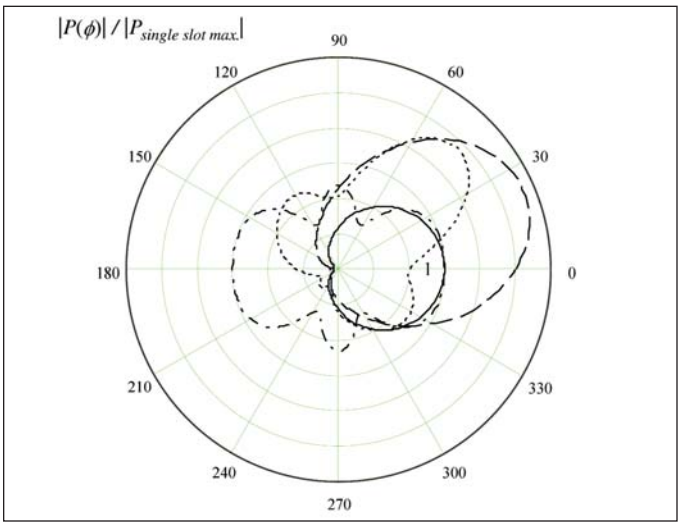

Figure 4(a) · Radiation patterns for $\phi_1 = 0$, $2\theta_1 = \theta_0$, $a = 0.358\lambda_0$, $b = 0.4217\lambda_0$, $\varepsilon_r = 4$ and $\mu_r = 1$, ---- one slot, · · · · $2\theta_2 = \theta_0$, $\phi_2 = \pi / 4$, - - - - $2\theta_2 = \theta_0$, $\phi_2 = \pi / 2$, -·-·-·- $2\theta_2 = \theta_0$, $\phi_2 = \pi$.

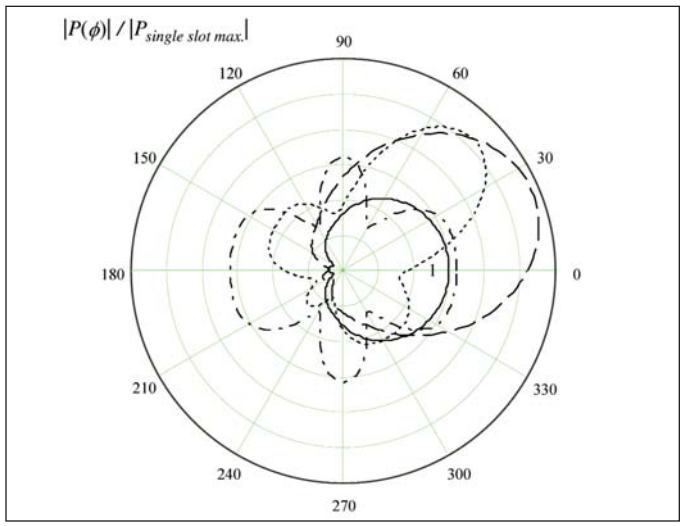

Figure 4(b) · Radiation patterns for $\phi_1 = 0$, $2\theta_1 = \theta_0$, $a = 0.358\lambda_0$, $b = 0.4217\lambda_0$, $\varepsilon_r = 1$ and $\mu_r = 4$, ---- one slot, · · · · $2\theta_2 = \theta_0$, $\phi_2 = \pi / 4$, - - - - $2\theta_2 = \theta_0$, $\phi_2 = \pi / 2$, -·-·-·- $2\theta_2 = \theta_0$, $\phi_2 = \pi$.

generally smaller and approximately unchanging up to $b = 2.15\ \lambda_0$ for all curves. Also, in Figure 3(b) the conductance is calculated for $\phi_1 = 0, 2\theta_1 = 2\theta_2 = \theta_0, \phi_2 = \pi / 4, \pi / 2$ and π, $\varepsilon_r = 4$, $\mu_r = 1$ and $a = 2\lambda_0$. We can see that the common shape is maintained but with smaller levels and the surface wave peaks are not changed.

The far field pattern expressed in equation (13) is calculated in Figure 4 and all patterns are normalized to the maximum value of the single slot case. Figure 4(a) shows a polar plot of the field pattern for one slot compared to two slots for $\phi_1 = 0$, $2\theta_1 = 2\theta_2 = \theta_0$, $\phi_2 = \pi / 4$, $\pi / 2$ and π, $\varepsilon_r = 4$, $\mu_r = 1$, $a = 0.358\lambda_0$ and $b = 0.4217\lambda_0$. As shown, the field is improved and a symmetry is produced around $\phi = \pi / 2$ caused by the two slots. In Figure 4(b), the field pattern is also illustrated for the same parameters except $\varepsilon_r = 1$ and $\mu_r = 4$. As expected, the radiation is also enhanced with a symmetry around $\phi = \pi / 2$.

The effects of slot size to radiation patters are shown in Figure 5 compared to the single slotted cylinder. A polar plot of the far field pattern is shown in Figure 5(a) for $\phi_1 = 0$, $\phi_2 = \pi$, $2\theta_1 = \theta_0$, $2\theta_2 = 2\theta_0$ and $4\theta_0$, $\varepsilon_r = 4$, $\mu_r = 1$, $a = 0.3\lambda_0$ and b = $0.45\lambda_0$. Also, in Figure 5(b), patterns are shown for the same parameters except $\varepsilon_r = 1$ and $\mu_r = 4$. One can observe that the patterns are highly enhanced as the slot size increase.

The radiated power expressed in equation (18) is plot-

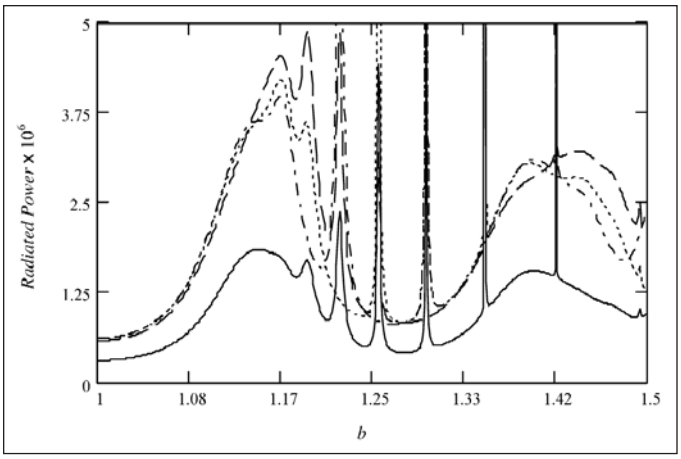

Figure 6(a) · Radiated power versus coating thickness for $\phi_1 = 0$, $2\theta_1 = 2\theta_2 = \theta_0$, $\varepsilon_r = 4$, $\mu_r = 1$, and $a = 1\lambda_0$, ---- one slot; - - - - $\phi_2 = \pi / 4$; · · · · $\phi_2 = \pi / 2$; -·-·-·- $\phi_2 = \pi$.

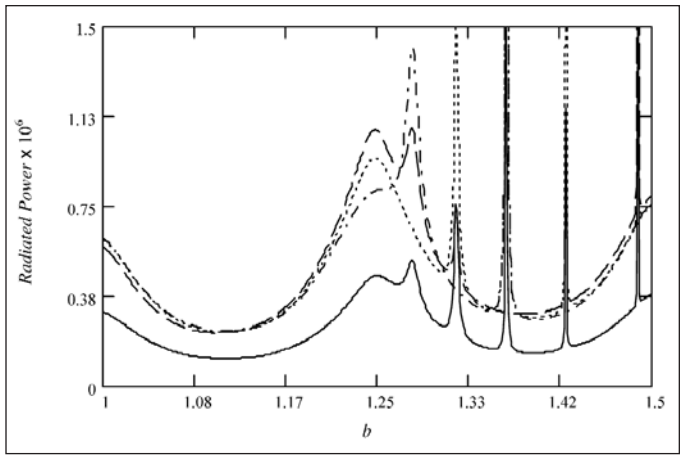

Figure 6(b) · Radiated power versus coating thickness for $\phi_1 = 0$, $2\theta_1 = 2\theta_2 = \theta_0$, $\varepsilon_r = 1$, $\mu_r = 4$, and $a = 1\lambda_0$, ---- one slot; - - - - $\phi_2 = \pi / 4$; · · · · $\phi_2 = \pi / 2$; -·-·-·- $\phi_2 = \pi$.

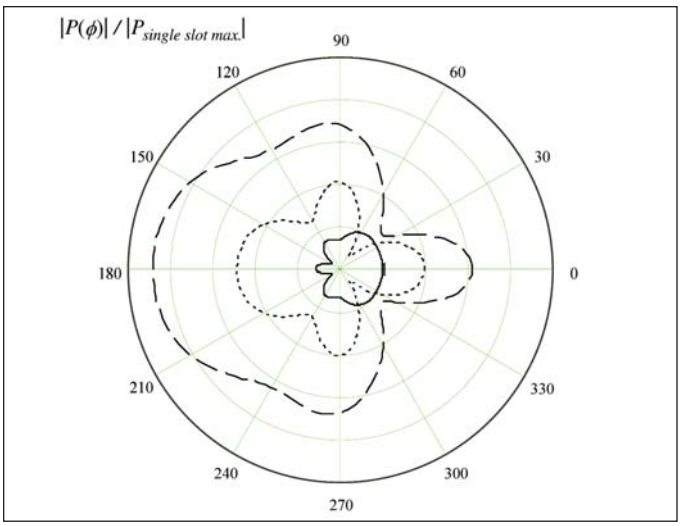

Figure 5(a) · Radiation patterns for $\phi_1 = 0$, $\phi_2 = \pi$, $2\theta_1 = \theta_0$, $a = 0.3\lambda_0$, $b = 0.45\lambda_0$, $\varepsilon_r = 4$ and $\mu_r = 1$; ---- one slot; · · · · $2\theta_2 = 2\theta_0$; - - - - $2\theta_2 = 4\theta_0$.

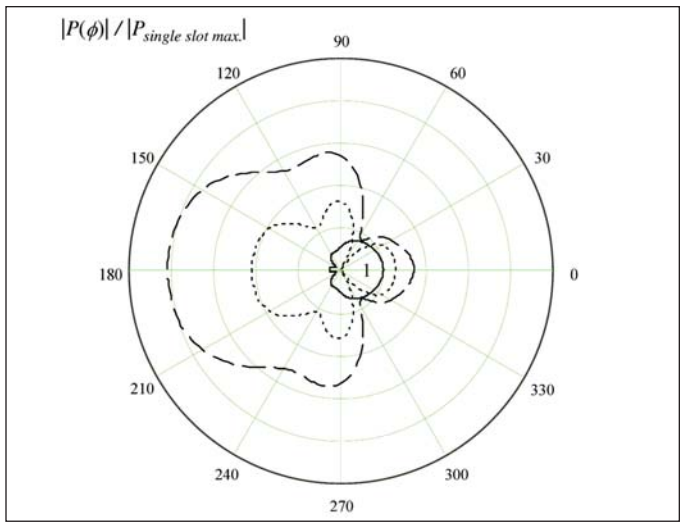

Figure 5(b) · Radiation patterns for $\phi_1 = 0$, $\phi_2 = \pi$, $2\theta_1 = \theta_0$, $a = 0.3\lambda_0$, $b = 0.45\lambda_0$, $\varepsilon_r = 1$ and $\mu_r = 4$, ---- one slot; · · · · $2\theta_2 = 2\theta_0$; - - - - $2\theta_2 = 4\theta_0$.

ted versus the coating thickness in Figure 6 compared to the single slotted cylinder. In Figure 6(a), the total power in the equatorial plane at $r \to \infty$ is shown for $\phi_1 = 0$, $\phi_2 = \pi / 4$, $\pi / 2$ and π, $2\theta_1 = 2\theta_2 = \theta_0$, $\varepsilon_r = 4$, $\mu_r = 1$, $a = 1\lambda_0$. For the same parameters except for $\varepsilon_r = 4$ and $\mu_r = 1$ the radiated power is plotted in Figure 6(b). As expected, more power is radiated from the two slotted cylinder than the single slotted cylinder. Also, the radiated power and the associated resonance peaks are almost the same regardless of the position of the second slot.

Additionally, the total radiated power as $r \to \infty$ is plotted in Figure 7 versus the size of the second slot in degrees. All curves are normalized to P_{eq0}, the equatorial power for $2\theta_2 = 0$. In Figure 7(a), the total power is shown for $\phi_1 = 0$, $\phi_2 = \pi / 4$, $\pi / 2$ and π, $2\theta_1 = \theta_0$, $\varepsilon_r = 4$, $\mu_r = 1$, $a = 1\lambda_0$ and $b = 2\lambda_0$. Also, for the same parameters except for $\varepsilon_r = 4$ and $\mu_r = 1$ the radiated power is plotted in Figure 7(b). In both cases the radiated power increases as the second slot size increases in approximately a nonlinear manner.

Conclusion

A solution for the problem of two axial slots in a circular cylinder covered by a dielectric material was derived. The TM case was considered and the radiated fields were represented in terms of an infinite series of

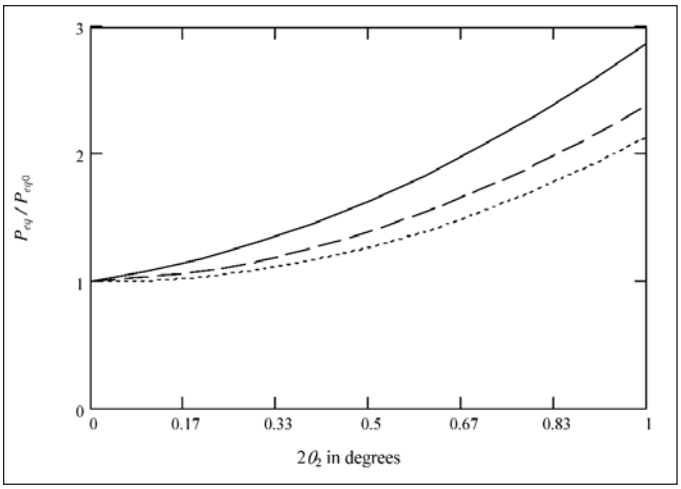

Figure 7(a) · Normalized radiated power versus slot size for $\phi_1 = 0$, $2\theta_1 = \theta_0$, $\varepsilon_r = 1$, $\mu_r = 4$, $a = 1\lambda_0$, and $b = 2\lambda_0$; – – – – $\phi_2 = \pi / 4$; - - - - $\phi_2 = \pi / 2$; · · · · $\phi_2 = \pi$.

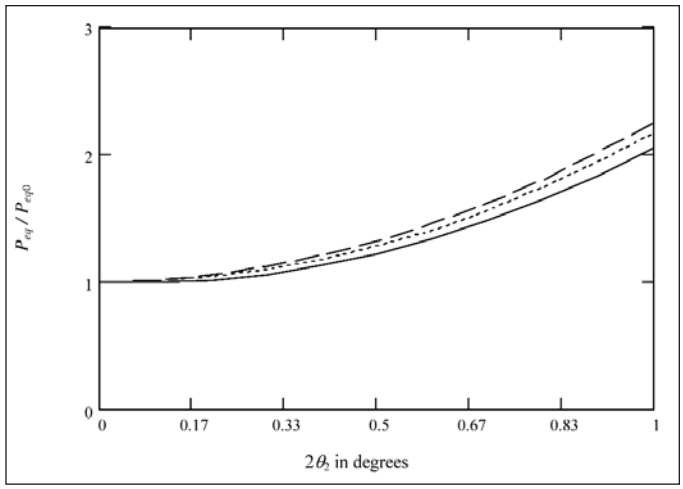

Figure 7(b) · Normalized radiated power versus slot size for $\phi_1 = 0$, $2\theta_1 = \theta_0$, $\varepsilon_r = 4$, $\mu_r = 1$, $a = 1\lambda_0$, and $b = 2\lambda_0$; – – – – $\phi_2 = \pi / 4$; - - - - $\phi_2 = \pi / 2$; · · · · $\phi_2 = \pi$.

cylindrical waves. The solution clarified the consequences of two slots with arbitrary size and position to the far field characteristics. Several changes were discovered to the antenna gain and the aperture conductance was obtained with lower values. An increase in the slot size can enlarge the radiated fields with some variations in the patterns. Also, the radiated power in the two slotted cylinder is greater than that in the single slotted cylinder. The radiated power increases as the size of the slot increases.

References

1. Barrow, W. L. (1936), "Transmission of electromagnetic waves in hollow tubes of metal", *Proceedings of the I. R E.,* Vol. 24, No. 10, pp. 1298-1328.

2. Harrington, Roger F. (2001), *Time–harmonic electromagnetic fields,* John Wiley & Sons, Inc., New York.

3. Hurd, R. A. (1956), "Radiation patterns of a dielectric-coated axially slotted cylinder," *Canadian Journal of Physics,* Vol. 34, pp. 638-642.

4. Mushref, Muhammad A. (2005), "Transverse magnetic scattering of two incident plane waves by a dielectric coated cylindrical reflector," *Central European Journal of Physics,* Vol. 3, No. 2, pp. 229-246.

5. Richmond, J. (1989), "Axial slot antenna on a dielectric-coated elliptic cylinder," *IEEE Transactions on Antennas and Propagation,* Vol. 37, No. 10, pp. 1235-1241.

6. Silver, S. and Saunders, W. (1950), "The external field produced by a slot in an infinite circular cylinder," *Journal of Applied Physics,* Vol. 21, pp. 153-158.

7. Sinclair, George (1948), "The patterns of slotted-cylinder antennas," *Proceedings of the I. R. E.,* Vol. 36, No. 12, pp. 1487-1492.

8. Wait, J. and Mientka, W. (1957), "Slotted-cylinder antenna with a dielectric coating," *Journal of Research of the National Bureau of Standards,* Vol. 58, No. 6, pp. 287-296.

9. Wait, James R. (1988), *Electromagnetic radiation from cylindrical structures,* Peter Peregrinus Ltd., London.

Author Information

Muhammad A Mushref was born in Almadeenah, Saudi Arabia. He received a BSc degree in Electrical Engineering from King Fahd University, Saudi Arabia, in 1991. In 1999, he completed an MSc degree in Data Communication Systems from Brunel University, UK and a further MSc degree in Computer Based Information Systems from the University of Sunderland, UK. In 2006, he received an MSc degree in Nuclear Engineering from King Abdulaziz University, Saudi Arabia. He also completed an MBA degree from the University of Leicester, UK in early 2009. Mr Mushref is a Chartered Engineer (CEng), an Incorporated Engineer (IEng) and a Chartered Information Technology Practitioner (CITP) with the Engineering Council, UK. He has 17 years experience working in various areas of communication and information technology and has developed and applied a wide knowledge of engineering and management in several supervisory positions. His research interests include computational electromagnetics and antenna analysis and design. He can be reached at: mmushref@yahoo.co.uk